

Quasi-ballistic scattering in quantum point contact systems

This article has been downloaded from IOPscience. Please scroll down to see the full text article.

1997 J. Phys.: Condens. Matter 9 673

(<http://iopscience.iop.org/0953-8984/9/3/007>)

View [the table of contents for this issue](#), or go to the [journal homepage](#) for more

Download details:

IP Address: 171.66.16.207

The article was downloaded on 14/05/2010 at 06:09

Please note that [terms and conditions apply](#).

Quasi-ballistic scattering in quantum point contact systems

Anna Grincwajg[†], G Edwards and D K Ferry

Center for Solid State Electronics Research, Arizona State University, Tempe, Arizona 85287-6206, USA

Received 16 August 1996

Abstract. Two scattering models are investigated in quasi-ballistic quantum point contact systems; a model with a few point scattering centres versus the Anderson model with on-site disorder. An exact, recursive Green's function technique is used to obtain magneto-transport quantities such as the conductance fluctuation amplitude and the correlation function. In the quasi-ballistic regime, the two models are not equivalent. The Anderson model can reproduce the same fluctuation amplitude as the 'few-scatterer' model, but fails to reproduce the correlation field. When the number of impurities in the 'few-scatterer' case is increased towards the diffusive regime, the two models agree well both on the fluctuation amplitude and correlation field. Further, we find that the correlation field in the Anderson model depends dramatically on disorder strength, when moving from the ballistic to the diffusive regime. The importance of the impurity positions in the 'few-scatterer' model is also investigated.

1. Introduction

Electron transport in mesoscopic systems has been intensely investigated during the past decade. One of the issues that has received much attention is conductance fluctuations. These fluctuations, which result from interference between different electron paths, have been observed in a variety of systems, such as metallic rings and wires [1, 2]. In the *diffusive* transport regime, where there exists an established theory, these fluctuations are called 'universal' (UCFs) because their amplitude is always of the order of e^2/h , independent of sample size or degree of disorder [3–5]. Recently, attention has been turned towards *ballistic* systems. Experiments have been performed on ballistic metallic point contacts [6–10], where conductance fluctuations of non-universal amplitude were measured. Theoretical calculations of conductance fluctuations in the quasi-ballistic regime have also been presented [7, 11–14].

In the quasi-ballistic regime, only a few impurities typically are present in the active phase coherent region. However, there are several examples in the literature where transport properties in the quasi-ballistic regime are calculated using the Anderson model with on-site disorder [11, 13, 14]. In the Anderson model, the entire system is discretized on a lattice, and disorder is incorporated by letting the energy of each lattice site vary randomly. The potential energy landscape is therefore a dense population of 'spikes', where the amplitude of the site energy variation reflects the disorder strength. Although this model has been very useful when describing localized and diffusive systems, it is indeed questionable to what extent it reflects the true nature of quasi-ballistic systems.

[†] Present address: Ericsson Microwave Systems AB, Bergfotsgatan 2, S-431 84 Mölndal, Sweden.

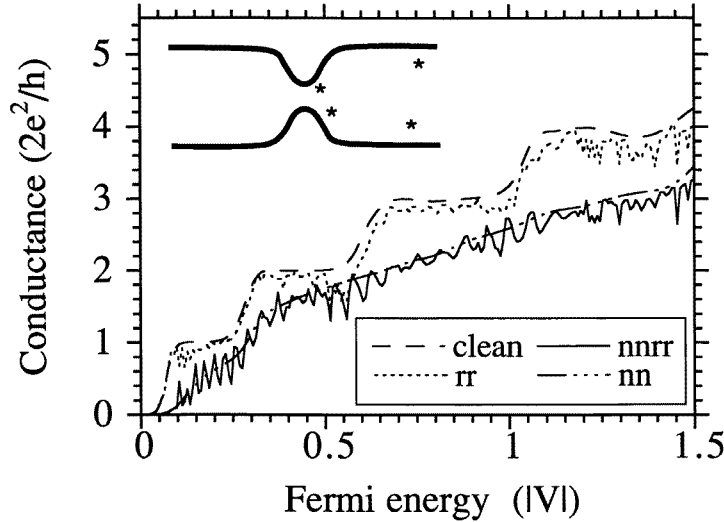


Figure 1. The inset shows the microstructure model geometry: a smooth two-dimensional quantum point contact connected to long leads. The positions of the few localized scatterers are marked with asterixes. The plot shows conductance as a function of Fermi energy, at $B = 0$, for three different impurity configurations, and the ‘clean’ case without impurities. In the case with two remote scatterers (rr), conductance fluctuations occur, while the two near scatterers (nn) act mainly as blockers, reducing the conductance. The situation with two near and two remote scatterers (nnrr) results both in strong conductance fluctuations and a reduction of the conductance.

In the present work, we compare the traditional Anderson model with a model including only a few localized scatterers. Our two-dimensional geometry consists of a smooth quantum point contact connected to long leads. A numerical calculation is performed to obtain magneto-transport properties such as the conductance fluctuation amplitude δg and the correlation function $F(\Delta B)$. In particular, we make connection to the work of [7], where non-universal conductance fluctuations in a ballistic metallic point contact were measured and successfully described by a theory including a few localized scatterers. We find that although the Anderson model can give the same result as the ‘few-scatterer’ model for the conductance fluctuation amplitude, it fails to reproduce the correlation field B_c in the quasi-ballistic regime. However, when the number of impurities in the ‘few-scatterer’ case is increased towards the diffusive regime, the two models agree well on both the fluctuation amplitude and correlation field. We also investigate the importance of the positions of the few localized scatterers, following the concepts of *near* and *remote* scatterers of [7]. We show that ‘near scatterers’, i.e. those located close to the orifice, act as blockers. They reduce the overall conductance significantly but do not lead to conductance fluctuations. The remote scatterers, on the other hand, result in strong conductance fluctuations but have a weak influence on the overall conductance.

2. The model

The microstructure geometry considered is a two-dimensional smooth quantum point contact connected to long leads, as shown in the inset of figure 1. We take the geometry to be smooth in order to avoid resonances and other interference effects resulting from sharp

geometrical features, an effect common in many numerical calculations. However, since our smooth geometry is discretized on a lattice, there is inevitably a certain amount of ‘surface roughness’ present, but the effect is found to be negligible for the energy range we consider.

The incorporation of long leads connected to the quantum point contact is an important issue [15–17]. In real experiments, any ballistic constriction must be connected to macroscopic reservoirs. If the temperature is sufficiently low, the phase coherent region will contain both the constriction and part of the leads, and it is important to treat the constriction and the contacts as one single system [11]. We include the long leads in our system, and find that impurities that are far from the constriction have a strong influence on the transport characteristics.

The quantum point contact geometry of figure 1 is, in our treatment, discretized on a square lattice. The laterally confining potential is introduced by letting the site energy be very large in regions inaccessible to the electrons (hard-wall boundary conditions). Throughout the paper, we will measure all energies in units of the tight-binding hopping energy $|V| = \hbar^2/2m^*a^2$ where a is the lattice constant. All lengths will be measured in units of the lattice constant, i.e. number of sites. If the lattice constant is much smaller than the Fermi wavelength, $\lambda_F/a \gg 1$, we are in the parabolic part of the energy band, and the lattice model is assumed to give a good description of the true continuum system. We have chosen the Fermi energy to be $E_F = 0.98|V|$ (if not specified otherwise), which corresponds to the ratio $\lambda_F/a = 6.34$. Our model is thus expected to describe a continuum system quite well. The chosen Fermi energy value corresponds to three propagating modes through the narrow part of the constriction.

The overall length and width of the geometry is denoted by L and W respectively, and the length and width of the smooth constriction is denoted by L_c and W_c . The width dependence $D(x)$ of the constriction is, with the x -coordinate being zero at the centre of the constriction,

$$D(x) = W + (W_c - W) \exp(-4x^2/L_c^2). \quad (1)$$

The parameter values are taken to be $L = 200$, $W = 20$, $L_c = 15$, and $W_c = 10$.

When modelling the ‘few-scatterer’ situation, we let the site energy be very large at the lattice sites corresponding to the positions of the scatterers (marked with asterixes in the inset of figure 1). This approach is equivalent to using a delta-function scattering potential. In the Anderson model, on the other hand, *each* site energy is taken to vary randomly (with a uniform distribution), within an energy interval $\pm u/2$, where u is the disorder strength.

The calculations are carried out using the recursive single-particle Green’s function technique [18–22]. Relations between the Green’s functions and the \mathbf{S} matrix of the system are employed [23], which allow the conductance to be calculated from the generalized multi-channel Landauer formula. The presence of a magnetic field, perpendicular to the plane of the constriction, is incorporated by means of a Peierls’ phase factor. Throughout the paper, the magnetic field strength will be measured in units of the frustration, $f = eBa^2/hc$, i.e. flux per unit cell. All calculations are performed in the weak- B -field limit, so the cyclotron radius is considerably larger than the narrowest part of the constriction. Also, care has been taken to exclude artifacts due to the underlying lattice, which occur when a B -field is present. In the cases where statistical averaging is performed, we average over the B -field range in the ‘few-scatterer’ model, and over 100 different disorder configurations in the Anderson model. According to the ergodic hypothesis, these two averaging procedures are equivalent. Finally, to ensure numerical reliability of our computational scheme, we require that current conservation holds to a tolerance of 1×10^{-6} .

3. Results and discussion

The aim of this work is to compare the traditional Anderson model with a model including a few localized scatterers. In spite of the fact that the impurity distribution in the quasi-ballistic regime has a much closer resemblance to a model with a few delta-function type scatterers than the Anderson model, the latter recently has been used in several works [11, 13, 14] to describe quasi-ballistic transport.

In our investigation, we make connection to the work of [7], where a theory based on a few localized scatterers successfully described the experimental data. In that work, non-universal conductance fluctuations, two orders of magnitude smaller than e^2/h , were measured as a function of magnetic field or voltage in a metallic 3D ballistic point contact. The authors presented a wave-optical description of the interference, showing that contributions from specific electron trajectories were responsible for the fluctuations observed. It was shown that a *combined interference* effect reproduced the data very well; one wave is confined in a region near the contact while the other is extended far into the electrode. Therefore, a model with a few localized scatterers in appropriate positions is expected to give rise to interference paths similar to those considered in that model.

We have adopted the concept of *near* and *remote* scatterers, and consider a situation with two near and two remote scatterers described by delta-function type potentials, as shown in the inset of figure 1. This is a model that closely corresponds to that of [7]. However, we perform a numerical calculation, taking into account scattering events of all orders, while the analytical calculation of [7] is based on perturbation theory. It is therefore also of interest to compare these two approaches.

3.1. The ‘few-scatterer’ model

We start by investigating the ‘few-scatterer’ model, where the positions of the impurities are as shown in the inset of figure 1. The conductance as a function of Fermi energy (or equivalently the gate voltage) at $B = 0$ is plotted in figure 1. In the ‘clean’ case, i.e. without impurities, the conductance steps are well defined and slightly rounded. The rounding of the steps is expected in a smooth geometry like this, due to quantum mechanical tunnelling through the thin top part of the sub-band potential each time a new mode threshold is approached. First, we consider the case when only the two ‘remote’ scatterers are present, labelled with the abbreviation ‘rr’. Conductance fluctuations are seen to be superimposed on the well preserved quantized steps, while the total conductance is only slightly reduced. The fluctuations result from trajectories involving the remote scatterers and the orifice boundary.

In the case of only two ‘near’ scatterers, denoted by ‘nn’, a dramatic difference occurs: the overall conductance is strongly reduced and conductance fluctuations are not visible. In other words, the near scatterers act as ‘blockers’, reflecting a large fraction of the incoming electrons. The conductance reduction is in agreement with known results for quasi-ballistic point contacts; i.e. the relative reduction is proportional to the relative area of the orifice being ‘shadowed’ by the scatterers. In the present model situation, with strong scatterers close to the orifice and a small number of propagating modes, the ‘shadowing’ effect is very strong. Further, since the electrons are reflected in very close proximity to the orifice, the typical correlation energies for interference fluctuations are so large that interference effects are not visible here.

Finally, we consider the case with two near *and* two remote scatterers, denoted by ‘nnrr’. The result is essentially a superposition of the two previous cases; the near scatterers still act as blockers, reducing the overall conductance, but the presence of the

remote scatterers introduces strong conductance fluctuations. These fluctuations result from scattering trajectories involving both the remote and the near scatterers. As we will see later, the presence of the near scatterers plays another important role, affecting the amplitude of the fluctuations. Of course, scattering at the orifice boundary also plays a significant role here.

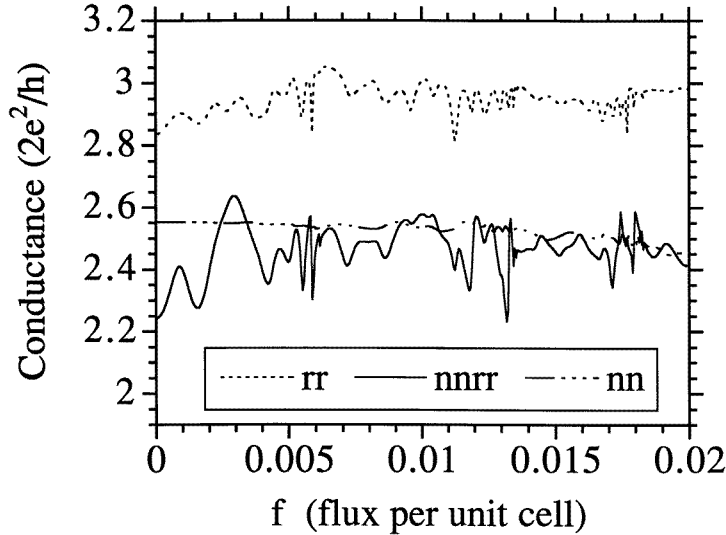


Figure 2. Conductance as a function of weak magnetic field, for the three different impurity configurations. The fluctuation characteristics for each impurity configuration are analogous to those of figure 1.

In figure 2, we plot the conductance for the same three impurity configurations, the ‘rr’, ‘nn’, and ‘nnrr’ cases, as a function of magnetic field. The Fermi energy is $0.98 |V|$, so we have three propagating modes through the orifice and are in the parabolic part of the band. The flux per unit cell is in the range $0 < f < 0.02$, which corresponds to the weak- B -field limit. It is seen that the fluctuation characteristics are equivalent to the case of figure 1 where the Fermi energy was varied, which is as expected. The configurations which contain remote scatterers exhibit conductance fluctuations, while the case with only near scatterers mainly reduces the conductance. In the two cases where near scatterers are present, the conductance is significantly reduced.

We have also calculated the average conductance $\langle g \rangle$ and the fluctuation amplitude δg for the two impurity configurations ‘rr’ and ‘nnrr’. The root mean square fluctuation amplitude is defined as $\delta g \equiv \langle (g - \langle g \rangle)^2 \rangle^{1/2}$, where the brackets denote averaging, here taken over the B -field interval. The result is the following: ‘rr’, $\langle g \rangle = 2.95$, $\delta g = 0.044$; ‘nnrr’, $\langle g \rangle = 2.46$, $\delta g = 0.078$. Thus, the addition of near scatterers to the remote scatterer case increases the fluctuation amplitude by a factor of approximately two. This result is in good qualitative agreement with that of [7], where it was found that a near trajectory causes a significant enhancement of the fluctuations. We wish to point out that only qualitative comparisons can be made with the results of [7], since in the experimental situation the number of modes is of the order of 10^3 , while in our model we have only three propagating modes. Further, the experiment is carried out on a strictly 3D metallic point contact, while the effective dimensionality of our model is somewhere between 2D and 1D.

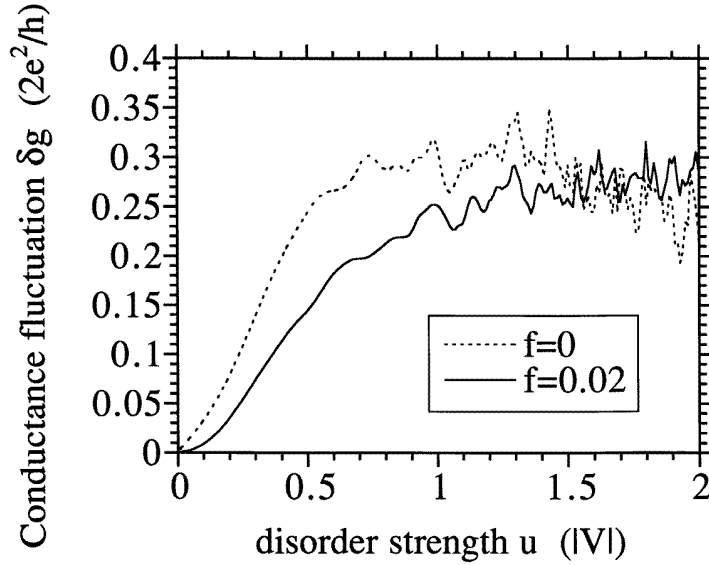


Figure 3. Conductance fluctuation amplitude δg versus disorder strength, for the B -field strengths $f = 0$ and $f = 0.02$, in the Anderson model with on-site disorder. The fluctuation amplitude increases monotonically in the quasi-ballistic regime from zero up to a saturation value, and fluctuates around a constant value in the diffusive (universal) regime.

3.2. The Anderson disorder model

Next we turn our attention to the Anderson model with on-site disorder. We use the same geometry as in figure 1 (inset), but here introduce the disorder potential on each site on the lattice. In figure 3 we show the conductance fluctuation amplitude δg versus disorder strength u , for zero flux and for $f = 0.02$. The disorder strength varies from zero up to $u = 2$. It is seen that the fluctuation amplitude increases monotonically from zero up to a saturation value, the saturation indicating that we have reached the universal (diffusive) regime. The crossover from the ballistic to the diffusive regime has been investigated in detail elsewhere [14], so we do not go into detail here.

The well known result that a magnetic field suppresses conductance fluctuations in the diffusive regime is clearly seen as the difference between the two curves of figure 3. Interestingly, the curves cross at disorder strength $u = 1.5$. In other words, the magnetic field suppresses the fluctuations in the quasi-ballistic and diffusive regime, but enhances them when the localized regime is entered. The same effect has been observed also by the authors of [12].

It is useful to relate the disorder parameter u to the elastic scattering length l , and in a 2D system we have

$$l = (6\lambda_F^3/\pi^3 a^2)(E_F/u)^2. \quad (2)$$

From this relation, the disorder strength $u = 0.5$ corresponds to $l \approx 170$ and $u = 1.5$ corresponds to $l \approx 20$. The total length of our system is $L = 200$, so we see that the fluctuation amplitude increases only while we are in the quasi-ballistic regime, which can be defined as the regime where $l \geq L$.

The almost linear relation between fluctuation amplitude and disorder strength in the quasi-ballistic regime implies that, by choosing the right disorder strength, the Anderson

model can reproduce any fluctuation amplitude smaller than the universal value. To make connection to the ‘few-scatterer’ model we note that the fluctuation amplitude $\delta g = 0.078$, obtained above for the ‘nnrr’ case, corresponds to the disorder strength $u = 0.3$ in the Anderson model. The next issue to investigate is how well the two different scattering models agree on estimating the typical fluctuation period.

3.3. Comparison of correlation functions

An important quantity for characterizing conductance fluctuations is the correlation function $F(\Delta B)$, defined as

$$F(\Delta B) = \langle (g(B) - \langle g(B) \rangle)(g(B + \Delta B) - \langle g(B + \Delta B) \rangle) \rangle \quad (3)$$

where g is the conductance and the brackets denote ensemble averaging. The correlation field B_c is defined as the half-width of the correlation function, $F(B_c) = F(0)/2$, and corresponds to the field strength required in order to increase the enclosed flux in a typical phase coherent area by one quantum. It can be loosely interpreted as the typical conductance fluctuation period. In the following notation we will replace ΔB by Δf , since we measure the magnetic field strength in terms of the frustration f .

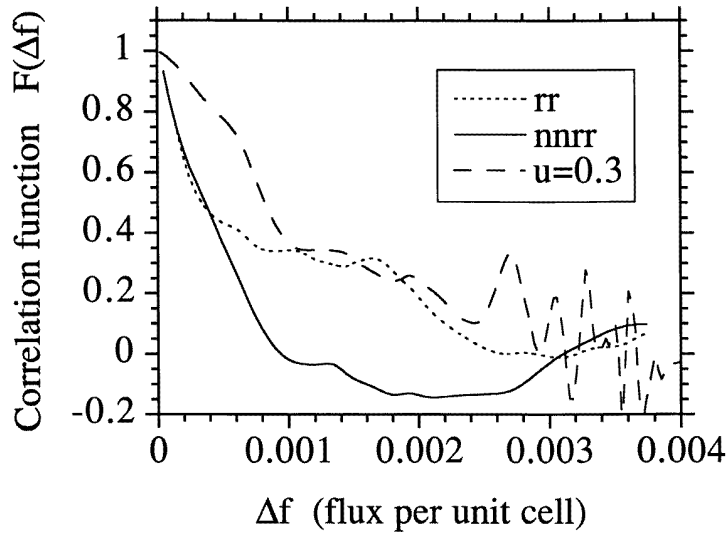


Figure 4. The normalized correlation function $F(\Delta f)$ for three different cases: the ‘rr’ and the ‘nnrr’ impurity configurations in the ‘few-scatterer’ model, and the Anderson model with disorder strength $u = 0.3$. The ‘rr’ and ‘nnrr’ configurations give the same correlation field, while the Anderson model correlation field is approximately twice as large.

In figure 4, we have calculated the normalized correlation function $F(\Delta f)$ for three different cases: the ‘rr’ and the ‘nnrr’ impurity configurations in the ‘few-scatterer’ model, and the Anderson model with disorder strength $u = 0.3$. First of all, we see that the ‘rr’ and ‘nnrr’ configurations give almost exactly the same correlation field B_c . This is supported by [7], where it was found that the correlation field is mainly governed by the remote scatterers. It does indeed seem natural that, in the quasi-ballistic regime, the positions of the remote scatterers define the typical trajectory size. We also note that the line shape of the ‘nnrr’ correlation function, being linear also near $\Delta f = 0$, is in good agreement with the

experimental data of [7], while the Anderson model correlation function line shape is closer to the flat Lorentzian type. However, the correlation function for the Anderson model with disorder strength $u = 0.3$ (to match $\delta g = 0.078$ in the ‘nnrr’ case), produces a correlation field that is approximately a factor of two larger than the ‘few-scatterers’ case. A possible explanation of this will be discussed below.

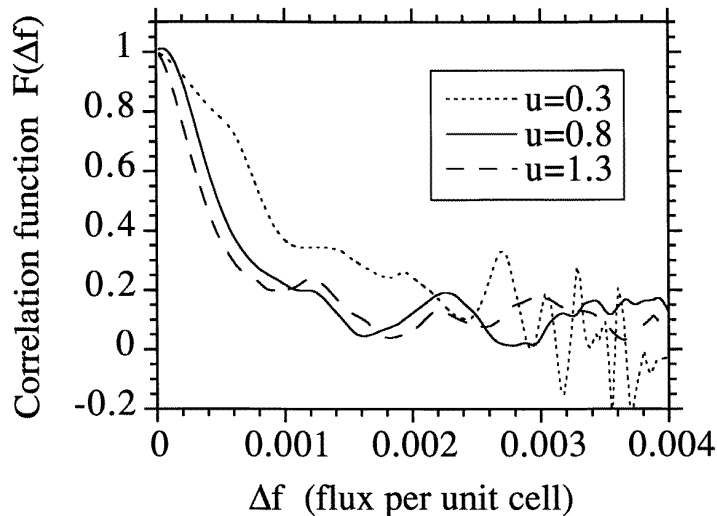


Figure 5. The normalized correlation function $F(\Delta f)$ for three different disorder strength values in the Anderson model. It is seen that the correlation field decreases with increasing disorder strength. The lineshape near $\Delta f = 0$ is of the flat Lorentzian type.

Finally, we are interested in calculating correlation functions for the Anderson model with different degrees of disorder. In figure 5, three correlation functions are shown, for disorder strength values of $u = 0.3, 0.8,$ and 1.3 . The corresponding elastic scattering lengths, calculated from (2), are $l = 526, 74,$ and 28 sites. The total length of our system is $L = 200$ sites. It is clearly seen that the correlation field decreases with increasing disorder strength. The line shape is similar for the different disorder strengths, being of the flat Lorentzian type near $\Delta f = 0$. We note that the shoulder is present, to differing degrees, in all three cases.

In figure 6, we show the correlation field B_c as a function of disorder strength, over the interval $0.3 < u < 2$. The general trend is the same as indicated in figure 5: the correlation field decreases with increasing disorder strength. Interestingly, there is a significant drop occurring at disorder strength $u \approx 0.8$, where the correlation field falls to approximately half of its value. After this sudden drop, there is a continuous decrease towards zero.

The decrease of correlation field with increasing disorder strength in the Anderson model can be explained as follows. The correlation field is inversely proportional to the (phase-coherent) area covered by closed electron trajectories. For weak disorder strengths, corresponding to the quasi-ballistic regime, the elastic scattering length is comparable to the system size. In the absence of a magnetic field, the probability of electron trajectories forming closed loops is therefore very small. However, for the magnetic field strength considered here, a weak trajectory bending occurs, making closed loops possible and thus leading to interference effects. This type of trajectory covers only a small part of the total system, and therefore the corresponding correlation field is large. However, when the disorder strength is increased towards the diffusive regime, the elastic scattering length

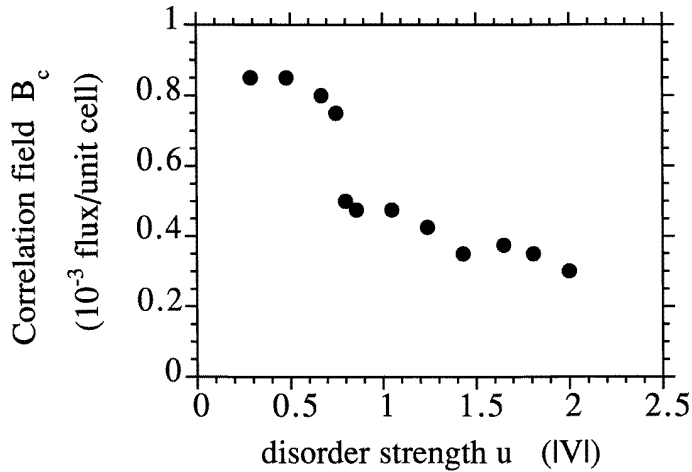


Figure 6. The correlation field B_c as a function of disorder strength in the Anderson model. The correlation field decreases with increasing disorder strength, and a significant drop occurs at disorder strength $u = 0.8$.

becomes considerably smaller than the system size. The number of closed loops is then large, and the corresponding trajectory covers a large part of the total system. This diffusive motion results in smaller correlation fields.

The above consideration also explains why the Anderson model, in the quasi-ballistic limit, produces a correlation field that is much larger than in the ‘few-scatterer’ case (figure 4). In the ‘few-scatterer’ case considered, the impurities are positioned so that a closed trajectory, covering a large part of the system, has a high probability of being realized. Therefore, the resulting correlation field will be considerably smaller than one that corresponds to the quasi-ballistic Anderson model, as discussed above.

It is interesting to compare the above dependence with the results of [7]. In that work, where only a few scatterers were considered, it was found that the correlation field B_c is given by $B_c \approx (h/e)/l^2$. In other words, the elastic scattering length l defines the typical trajectory size. If we apply this result to the Anderson model, using (2), we find that the correlation field should depend on disorder strength as $B_c \sim u^4$. This is certainly not in agreement with our results, even in the quasi-ballistic regime. We therefore conclude that the inelastic scattering length in the Anderson model, taken in the quasi-ballistic regime, is not a good measure of the typical trajectory size.

3.4. The ‘few-scatterer’ case with more impurities

So far we have, in the ‘few-scatterer’ case, considered a situation that does not allow us to introduce the concept of an elastic scattering length, since the number of impurities is very low. However, if the number of impurities is increased, an elastic scattering length can be defined, and we can thus make a more quantitative comparison with the Anderson model. We therefore now consider a situation with 15 randomly positioned impurities across the entire confinement of figure 1 (inset), the impurities being defined exactly in the same way as in the previous ‘few-scatterer’ case. The elastic scattering length can in this case be roughly estimated as $l \approx 20$ sites. In the Anderson model, an elastic scattering length $l \approx 20$ sites can be obtained, taking the disorder strength value to be $u = 1.5$ (using (2)).

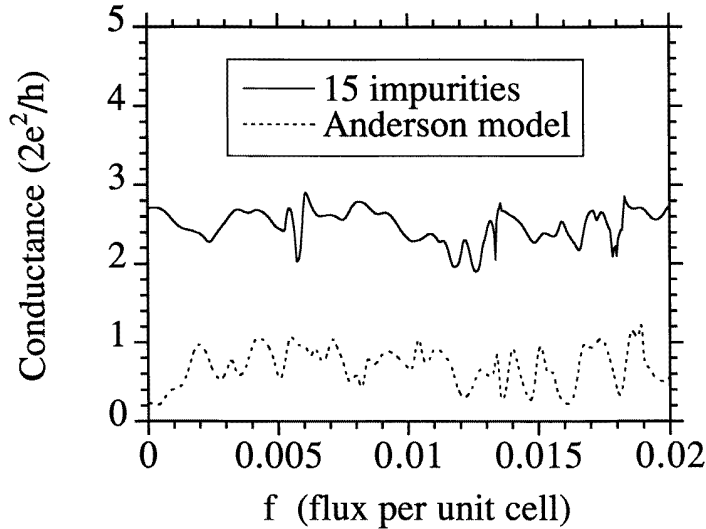


Figure 7. Conductance as a function of weak magnetic field. The case of 15 randomly positioned impurities is compared to the Anderson model with on-site disorder. The parameters are chosen so that the inelastic scattering length is the same in both models, $l \approx 20$ sites. The fluctuation amplitudes are found to be $\delta g = 0.20$ for the case with 15 impurities and $\delta g \approx 0.25$ for the Anderson model.

In figure 7, we plot the conductance as a function of magnetic field (weak- B -field limit), comparing the case with 15 impurities to the on-site disorder Anderson model with disorder strength $u = 1.5$. It is seen that the aperiodic fluctuations are similar in character, but the average conductance is significantly smaller in the Anderson model case. We have calculated the fluctuation amplitude δg in the case of 15 impurities by averaging over the B -field range of figure 7, with the result $\delta g = 0.20$. For the Anderson model case, the fluctuation amplitude can be obtained from figure 3, where δg versus disorder strength u is plotted. We find that the disorder strength $u = 1.5$ corresponds to $\delta g \approx 0.25$. Obviously, the two different scattering models give roughly the same fluctuation amplitude, as long as the corresponding elastic scattering length is the same.

In order to make the comparison complete, we must also investigate the correlation functions. In figure 8, we show the correlation functions $F(\Delta f)$ for the case with 15 impurities and the Anderson model with on-site disorder, $u = 1.5$. The agreement is very good for small Δf , almost down to $F = 1/2$. However, the line shape near $\Delta f = 0$ is different for the two models; the Anderson model correlation function is of the flat Lorentzian type, while the ‘few-scatterer’ model correlation function is nearly linear. For larger Δf , the Anderson model correlation function continues linearly down to smaller values, while the ‘few-scatterer’ model correlation function exhibits a shoulder before a further decrease.

4. Conclusions

We have compared the traditional Anderson disorder model to a model including only a few localized scatterers. The ‘few-scatterer’ model is assumed to be more realistic when modelling the quasi-ballistic regime, and has successfully been used to describe experiments

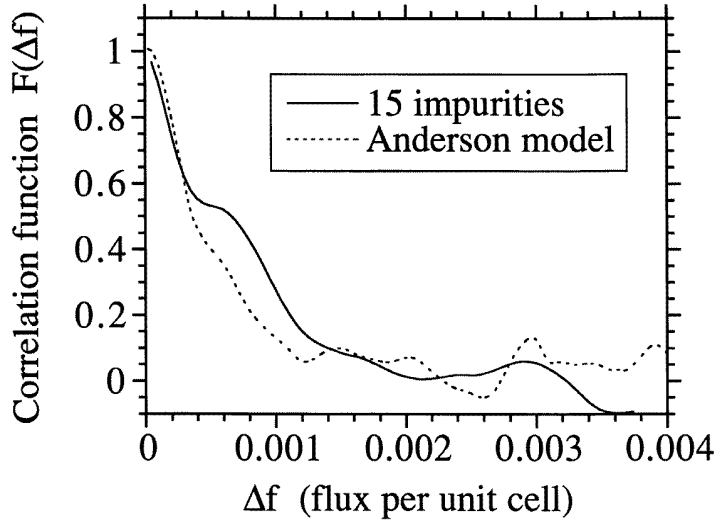


Figure 8. The normalized correlation function $F(\Delta f)$ for two situations: 15 randomly positioned impurities and the Anderson model with on-site disorder. The inelastic scattering length is the same in both models, $l \approx 20$ sites. It is seen that the two models agree quite well on estimating the correlation field.

[7]. We have performed an exact, numerical calculation of magneto-transport properties, considering a smooth quantum point contact geometry connected to long leads.

We find that the Anderson model can, with appropriately chosen disorder strength, reproduce any conductance fluctuation amplitude δg . Therefore, it can reproduce the very small fluctuation amplitudes found in quasi-ballistic systems. However, it does not give the same correlation field B_c or correlation function line shape as the ‘few-scatterer’ model in the quasi-ballistic regime. The reason is that the typical trajectory sizes are different in the two models. We also find that the correlation field in the Anderson model depends dramatically on disorder strength, when moving from the ballistic to the diffusive regime. Further we find that, when the number of impurities in the ‘few-scatterer’ case is increased towards the diffusive regime, the two models agree quite well both on the fluctuation amplitude and correlation field. We therefore conclude that the Anderson disorder model is not suitable for a complete description of conductance fluctuations in the quasi-ballistic regime.

We have also investigated the importance of the impurity positions in the ‘few-scatterer’ model. Impurities located near the orifice act mainly as ‘blockers’, reducing the overall conductance, while the remotely located impurities lead to significant conductance fluctuations. The presence of near scatterers enhances the fluctuation amplitude by a factor of two, a result that supports the theory of [7], where it was found that a combination of near and remote interference trajectories accurately describes the experimental situation.

Finally, it is worthwhile to speculate on the nature of the difference between the two correlation functions resulting from the two models, and recent experimental observations of fluctuations in ballistic quantum dots [24, 25]. In these experiments, a transition between regular and chaotic behaviour is assumed to have taken place, with this transition being signalled by the change in the weak-localization line shape. This change has been suggested in chaotic and regular dot systems [26, 27]. However, this behaviour has also been seen in single quantum point contacts [28, 29], a system quite different from the quantum dot, and

similar to the microstructure studied here. Dominance of a quantum dot by a single quantum point contact is well known [30], which suggests that the weak-localization behaviour, and its changes, might well be associated with the contacts rather than the central region of the dot [31]. Indeed, the strong similarity of the magnetic field behaviour of the correlation functions found here to that observed both in dots and single quantum point contacts suggests that a much deeper tie between the structures might well exist.

Acknowledgments

We are grateful to V I Kozub and J Caro for ideas and suggestions that initiated this work, and for most valuable discussions and comments during the completion of the project. AG acknowledges postdoctoral fellowships from the Swedish Research Council for Engineering Sciences (TFR), the Swedish Institute (SI) and the Ericsson ISS'90 foundation. GE and DKF acknowledge support from NEDO under the International Joint Research Program 'Nanostructures and Electron Waves Project' and from the Office of Naval Research.

References

- [1] Umbach C P, Washburn S, Laibowitz R B and Webb R A 1984 *Phys. Rev. B* **30** 4048
- [2] Webb R A, Washburn S, Umbach C P and Laibowitz R A 1985 *Phys. Rev. Lett.* **54** 2696
- [3] Stone A D 1985 *Phys. Rev. Lett.* **54** 2692
- [4] Altshuler B L 1985 *Pis. Zh. Eksp. Teor. Fiz.* **41** 530 (Engl. Transl. *JETP Lett.* **41** 648)
- [5] Lee P A, Stone A D and Fukuyama H 1987 *Phys. Rev. B* **35** 1039
- [6] Holweg P A M, Kokkedee J A, Caro J, Verbruggen A H, Radelaar S, Jansen A G M and Wyder P 1991 *Phys. Rev. Lett.* **67** 2549
- [7] Kozub V I, Caro J and Holweg P A M 1994 *Phys. Rev. B* **50** 15 126
- [8] Holweg P A M, Caro J and Kozub V I *Preprint*
- [9] Ralph D C, Ralls K S and Buhrman R A 1993 *Phys. Rev. Lett.* **70** 986
- [10] Murek U, Schäfer R and Langheinrich W 1993 *Phys. Rev. Lett.* **70** 841
- [11] Maslov D L, Barnes C and Kirzenow G 1993 *Phys. Rev. Lett.* **70** 1984; *Phys. Rev. B* **48** 2543
- [12] Tamura H and Ando T 1991 *Phys. Rev. B* **44** 1792
- [13] Higurashi H, Iwabuchi S and Nagaoka Y 1992 *Surf. Sci.* **263** 382
- [14] Grincwajg A, Edwards G and Ferry D K 1996 *Physica B* **218** 92
- [15] Engquist H L and Anderson P W 1981 *Phys. Rev. B* **24** 1151
- [16] Büttiker M 1988 *Phys. Rev. B* **38** 9375
- [17] Chandrasekhar V, Prober D E and Santhanam P 1988 *Phys. Rev. Lett.* **61** 2253
- [18] Lee P A and Fisher D S 1981 *Phys. Rev. Lett.* **47** 882
- [19] Baranger H U, DiVincenzo D P, Jalabert R A and Stone A D 1991 *Phys. Rev. B* **44** 10 637
- [20] Kawamura T and Leburton J P 1993 *Phys. Rev. B* **48** 8857
- [21] Czyczoll C and Kramer B 1979 *Solid State Commun.* **32** 945
- [22] Thouless D J and Kirkpatrick S 1981 *J. Phys. C: Solid State Phys.* **14** 235
- [23] Szafer A and Stone A D 1988 *IBM J. Res. Dev.* **32** 384
- [24] Chang A M, Baranger H U, Pfeiffer L N and West K W 1994 *Phys. Rev. Lett.* **73** 2111
- [25] Bird J P, Ishibashi K, Ferry D K, Newbury R, Olatana D M, Ochiai Y, Aoyagi Y and Sugano T 1997 *Surf. Sci.* at press
- [26] Jalabert R A, Baranger H U and Stone A D 1990 *Phys. Rev. Lett.* **65** 2442
- [27] Baranger H U, Jalabert R A and Stone A D 1993 *Phys. Rev. Lett.* **70** 3876
- [28] Taylor R P, Newbury R, Dunford R B, Coleridge P T, Sachrajda A S and Adams J A 1995 *Phys. Rev. B* **51** 9801
- [29] Katine R, Eriksson M A, Westervelt R M, Campman K L and Gossard A C 1997 *Superlatt. Microstruct.* at press
- [30] Kouwenhoven L P, van Wees B J, Kool W, Harmans C J P M, Staring A A M and Foxon C T 1989 *Phys. Rev. B* **40** 8083
- [31] Ferry D K, Akis R, Udipi S, Vasileska D, Pivin D P Jr, Connolly K M, Bird J P, Ishibashi K, Aoyagi Y, Sugano T and Ochiai Y 1997 *Japan. J. Appl. Phys.* at press